4th Imeko TC19 Symposium on Environmental Instrumentation and Measurements
Protecting Environment, Climate Changes and Pollution Control
June 3-4, 2013, Lecce, Italy

2D MEASUREMENTS OF PRIMARY SOOT DIAMETER IN DIFFUSION FLAMES BY TWO-DIMENSIONAL TIME RESOLVED LASER INDUCED INCANDESCENCE (2D TIRE-LII)

M. Potenza, F.Naccarato and A. de Risi

University of Lecce, Department of Engineering for Innovation
Via Monteroni - 73100 - Lecce
marco.potenza@unisalento.it

Abstract: Two dimensions primary soot diameter calculation in a laminar diffusion LPG flame by means of Laser Induced Incandescence (LII) is presented in present paper. LII is a high sensitive technique in which a high energy Nd-YAG laser sheet heats soot particles to a temperature of about 4000 K but without exceeding the sublimation temperature. Radiation from exited soot particles is acquired by means of an intensified CCD camera (low gate opening time of 10ns) synchronized with the laser pulse. By delaying the acquisition time with respect to laser pulse, LII signal decay as function of time has been reconstructed. Performing acquisition at two different wavelengths by means of two interferometric filters (Two color LII) a soot temperature behaviour (related to particles primary diameter) has been calculated. Using a self calibration method for optics and laser fluence and self-absorption corrections for LII signal, bi dimensional quantitative measurements can be achieved for soot dimensions and distribution. Thanks to a center- of-mass alignment of flame within corrected images at different time steps, it is possible to achieve the soot decay curve for each pixel of images, thus obtaining two dimensional soot primary particles visualization.

Keywords: 2D LII, Time Resolved LII, Laminar diffusion flame, Soot volume fraction.

1. INTRODUCTION

Soot produced during the combustion process of diffusion flames (e.g. gasoline and gas engines) is characterized by low dimension (about 10-30 nm diameter) [1] and consists of small carbon spheres connected together at point of contact to form more complex geometry (fractal-like branched geometry) [2, 3, 4]. These small particles are not easily detectable with conventional sampling or optical techniques. In the present work Laser Induced Incandescence (LII) technique has been applied to a laminar diffusion LGP flame (C_4H_{10} at 75 % and C_3 H_8 at 25 %) to measure soot particles primary diameter and volume fraction spatial distribution. LII is a diagnostic tool mainly used for spatially or temporally resolved measurement of particulate volume fraction and primary particle size in flames and combustion systems (i.e. engines and exhaust) [5]. LII is characterized by high sensitivity in soot detection and high precision in quantitative measurements. Soot emission intensity is related to the mass of carbon particles into the measurement specimen [6]. In particular peak intensity of the LII signal (the so called Prompt-LII) is proportional to soot volume fraction and the signal decay is related to particles dimension and surrounding gas temperature [7]. To heat soot rapidly near to sublimation temperature (about 4000 K), a high power pulsed laser sheet can be used. This technique can be applied both in one-dimension by means of a high sensitive photodiode and in two-dimensional visualization through an intensified CCD camera. Boiarciuc [8] and Snelling [9] used a photomultiplier together with a pin-hole to limit the acquisition of LII signal to a portion of flame. Moreover this method is not suitable for flames with high variability, such as acquisition directly in the combustion chamber. Using an intensified CCD camera it is possible to obtain the entire flame soot emission and to resolve the spatial soot distribution with a single shoot image (Spatially Resolved LII or SR-LII). To measure the soot properties and dimensions quantitatively, a calibration of the optical setup is required. Some authors suggest to calibrate the acquisition system by a cross correlation of the acquired signal with light extinction [10] or with signal from a known soot volume fraction source [11]. Snelling et al. [12] proposed an alternative self-calibration method based on the acquisition of the signal of a radiation source of known radiance. In this method, the detection system (CCD camera and filters) was calibrated a priori with a tungsten filament lamp of known temperature and radiance. The self calibration method allows performing the hardware calibration before flame acquisition. Calibration factor exclusively depends on the acquisition system and can be used for different fuels. Acquired LII signal is affected by experimental uncertainty because of the interaction between soot particles in flame and the radiation. In particular, two different kinds of interactions introduce high errors (about 12%) in soot quantitative measurements. The first, the so called self-absorption, occurs when radiation emitted by heated soot interacts with other soot particles in the optical

path between the laser sheet and the detector (ICCD) [13]. The second interaction is related to laser energy loss during flame crossing. Due to energy transfer to soot particles, a reduction of laser fluence along the flame path can be detected [7]. The dimension of primary particles can be calculated from the temporal variation of the LII signal. Temporal variation of soot characteristics is known as Time Resolved Laser Induced Incandescence or TIRE LII. In the present work a simultaneous SR-LII and TI-RE LII method for soot volume fraction and primary diameters calculation in a two dimensional image is proposed. To calculate 2D soot properties, a filtering process and a flame alignment in a fixed reference system was achieved. The pixel-to-pixel matching in time for the soot particles diameter calculation has been guaranteed by the alignment of the flame mass center.

2. THEORETICAL BACKGROUND

The calibration process converts the raw acquired signal of heated soot from pixel counts to emitted power expressed in W $m^{-2}sr^{-1}$ [14]. The calibration procedure allows quantitative measurements on soot volume fraction and particles diameters. Smallwood [15] proposed a self-calibration method to estimate heated soot temperature based on a two wavelengths signal measurement. For the CCD calibration purpose an ordinary tungsten lamp with steady known temperature was used. In particular, the calibration factor $\eta(\lambda)$ can be expressed as ratio between the tungsten lamp signal acquired by ICCD S_{Lamp} and the lamp spectral radiance R_{Lamp}. The calibration factor $\eta(\lambda)$ has been used to correct the flame signal acquired by means of the intensified CCD. For quantitative measurements, the collected signal expressed in counts has to be re-scaled with used ICCD gain (according to the camera datasheet) and the ICCD gate opening time (10ns in the present work). Moreover the ICCD spectral response (in blue region is about 30% less than the red component as well) and the interferometric filters transmittance (45% for blue and 55% of red) were used to correct acquired signal. A further correction factor depending on the solid angle of optics view was calculated. The radiated power from a single soot particle of primary diameter d_p into a solid angle of 4π, can be expressed as [15]

$$P_p(\lambda) = \frac{8\pi^3 c^2 h}{\eta(\lambda)\lambda^6} \frac{d_p^3}{(e^{\frac{hc}{k_b \lambda T}} - 1)} F(m_\lambda) \tag{1}$$

where c is the light velocity, h the Planck constant, k_b the Boltzmann constant, T the heated particle temperature, λ the pass-band interferometric filter wavelength and $F(m)$ absorption function depending on the complex refraction index of the soot [16].

The theoretical heated soot temperature can be expressed as ratio between the acquired LII signal at two different wavelengths (red at 635 nm and blue at 488 nm in the present work):

$$T = \frac{\frac{hc}{k_b}\left(\frac{1}{\lambda_2} - \frac{1}{\lambda_1}\right)}{ln\left(\frac{F(m_1)}{F(m_2)}\right) + ln\left(\frac{I_2 \lambda_2^6}{I_1 \lambda_1^6}\right)} \tag{2}$$

After a calibration and from the heated soot temperature, soot volume fraction has been obtained for each time using relation 3

$$f_v = I(\lambda) \frac{\lambda^6}{12\pi c^2 h F(m) w_b} \left(e^{\frac{hc}{k_b \lambda T}} - 1\right) \tag{3}$$

During the soot cooling phase, temperature difference between soot particles and surrounding gas decays exponentially. McCoy and Cha [17] proposed a formulation for the particles primary diameter as function of the characteristic decay time:

$$d_p = \frac{12 k_g \alpha \tau}{G c_p \rho_p \lambda_{MFP}} \tag{4}$$

where k_g is the thermal conductivity of the ambient gas, α is the so called thermal accommodation coefficient (equal to 0.26 [18]), G is a geometry-dependent heat transfer factor (equal to 22.064), λ_{MFP} is the molecular mean free path in the ambient gas, c_p and ρ_p are the specific heat and density of soot respectively [19]. The number of particles N_p can be calculated by means of the heated volume from relation $N_p = n_p (w_b A_p)$. Soot volume fraction and particles density is directly dependent from the LII signal, so a high precision calibration and flame alignment have to be reached for low error quantitative measurements

3. EXPERIMENTAL SETUP

In Figure 1 two-dimension time resolved LII experimental setup is shown. The diffusion LGP flame was produced by means of a co-annular circular burner with a diameter of fuel outlet of 6 mm. A ceramic honeycomb with holes diameters of 0.5 mm was inserted into the fuel orifice to stabilize the flame.

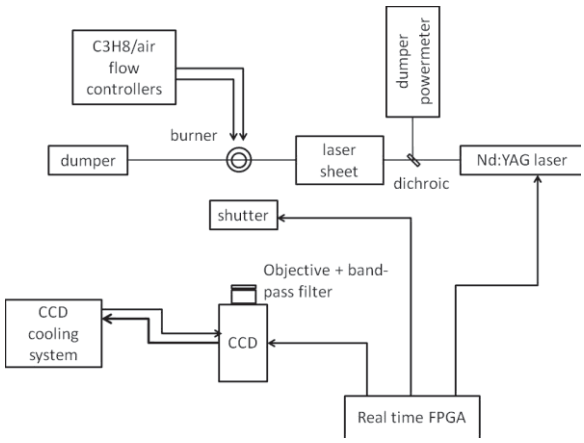

Figure 1: Experimental set-up for laser induced incandescence

A constant air flow enclosed the flame thus increasing its stability. Two mass flow meter/controllers (Brooks

Instruments 5850S/BC) regulated fuel and air flow at 2.2 cc/s and 117 cc/s respectively. The height of the produced flame was about 60 mm and the diameter at the base was 14 mm. As excitation source a Nd-YAG 10Hz pulsed laser (Quanta Ray PIV 400) with 400 mJ of energy in 8 ns pulse duration was used. A dichroic lens separated the 532nm wavelength while the rest of light spectrum was directed in a light power meter in order to ensure constant power. Laser beam was diverged by a spatial filter formed by a plane-concave lens (f=-6mm) and then filtered through a slit to achieve a laser sheet of rectangular section (about 500µ) and an uniform energy profile. LII signal was acquired by means of a water-cooled intensified CCD camera Andor iSTAR. To perform heated soot temperature measurement, CCD camera was equipped by a 25mm f/2.8 objective with two interchangeable interferometric filters at 488nm and 635nm with 10nm of FWHM for both. The gate opening time was set to 10 ns. A real time processor with a Field Programmable Gate Array (FPGA) on board provided the signal triggers for the laser Q-Switch and light pulse, shutter opening and CCD acquisitions. In order to measure the ICCD camera calibration curves at the two selected wavelengths (λ_1=488nm and λ_2=635nm), a calibrated tungsten lamp was used. The ordinary tungsten lamp was characterized by means of a monochromator Jobin-Yvone HR460 equipped with an intensified CCD camera Jobin-Yvone UV18F. The calibration method was proposed by Rosenkranz [20] and allows to characterize the lamp as function of temperature using the tungsten emissivity values [21]. To maximize LII signal and signal-to-noise ratio, the energy fluence curve was analyzed related to the soot particles conditions. Different heat loss and particles decay mechanism occur depending on laser fluence. Typically, three phases characterize soot behaviour with respect to laser energy [22, 23]: heating, graphitization and vaporization. As pointed out by Schulz et al.[22] due to high soot mass loos, vaporization regime is harmful for two-color LII particle sizing and quantitative measurements. A low-fluence regime between 120mJ/cm^2 and 200mJ/cm^2 is reasonable condition to avoid soot sublimation and volume reduction. For a value of laser fluence just above 200 mJ/cm^2 LII peak is fluence independent. In the present study, a fluence value of about 200 mJ/cm^2 was chosen to avoid soot sublimation and to increase the signal-to-noise ratio. A post processing of alignment and averaging was carried out on the acquired images, as reported below. This procedure was carried out for two different wavelengths (488 and 635 nm). In Figure 2, time evolution of the LII signal has been reported for both wavelengths. The graph was obtained with an integral over the image for each time step and applying all optical corrections. A few nanosecond rising part (due to laser pulse signal) of about 20 ns and a decreasing part of about 2µs due to soot cooling can be observed for both blue and red filtered data. The intensity of LII signal for a single wavelength is related to soot volume fraction (the higher the signal, the higher the soot volume fraction) while the decreasing shape is related to particles primary diameter (the slower the cooling rate, the bigger the diameter).

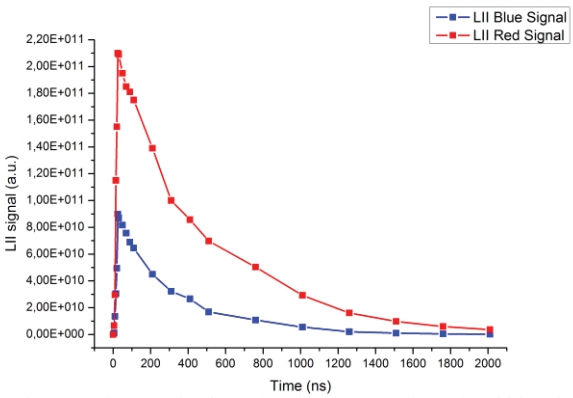

Figure 2 Time resolved LII signal (TIRE LII) for red and blue signals

3.1. IMAGES POST-PROCESSING AND ANALYSIS

For each time step the average of the 50 repetitions was calculated. To reduce the averaging error acquired images were aligned, rotated and over-lapped each other on the basis of their mass center for each time step. Mass center position was calculated after a flame edge contour detection. Each single repetition was filtered and perspectively corrected. Noise reduction was obtained by a filtering process in two phases: the first one was an adjacent points smoothing filter over 10 pixel length; the second one was a low-pass FFT filter with a normalized cut-off frequency of 0,125. A perspective calibration based on a calibration pattern template was applied to images in order to correct optics distortions and to correlate the pixel coordinates of the images to the real world dimensions. The inter-holes distance and the hole diameters of the calibration pattern are of 2 mm. Calibration pattern was positioned on the burner in the middle of flame position, in the same position of the laser sheet. In Figure 3 (a) images treatment process is briefly described while in Figure 3 (b) the calibration pattern is reported.

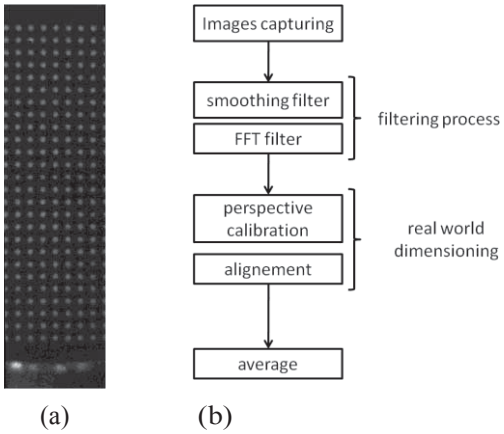

Figure 3: a) Synoptic of the images treatment process; b) perspective calibration pattern image.

A correction for laser fluence reduction through the flame was developed after images filtering and calibration. During flame crossing by laser sheet, indeed, the laser energy is transferred to soot particles heated below to sublimation

temperature. This phenomenon leads to an asymmetry in flame radial profile image. In Figure 4 a flame image affected by laser energy loss is reported. In particular, a signal attenuation is detectable in the laser propagation direction (from left to right) [7]. In Figure 4 can be distinguished three different zones in which the laser fluence reduction is evident.

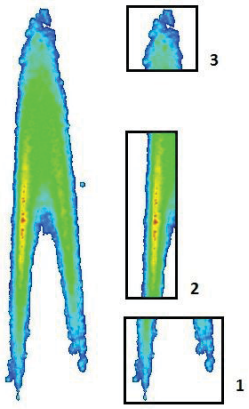

Figure 4: LII signal affected by laser power loss

The first is in the lower part of flame (sub-image 1 of Figure 4 on right) where the left part shows a longer queue than the right one. The second is evident in the central part of the image (sub image 2) where a higher intensity of LII signal is evident in the left part of flame; the third zone is in the upper part of flame (sub image 3) where a signal lack is presented in the right part: in this zone the laser power is no longer able to heat soot particles significatively and no LII signal can be detected. This behaviour of laser fluence along the optical path leads to a wrong volume fraction measurements in a bidimensional domain. To eliminate this kind of error, the radial profile has been interpolated linearly with the last square residuals method. In case of no laser power loss in flame crossing, the interpolation line should have a quasi-zero slope because of flame symmetry. For flame reported in Figure 4, instead, a negative slope was calculated. To obtain a laser fluence compensation and a symmetric LII signal with respect to the flame axis, the acquired image has been multiplied with the reversed interpolating line. Higher value of compensation (about 3%) have been found in the middle and upper part of flame where there is great volume fraction of soot and consequently high laser power absorption. Signal acquired by the ICCD is lower than the emitted radiation from heated soot as soot particles constitute an optical absorbing medium. This phenomenon introduces an error in soot volume fraction quantitative measurements and is known as self-absorption. To evaluate the amount of radiation absorbed by soot between heated particles and the collection system, light extinction method has been applied to the flame. To investigate the whole flame at a single wavelength, a light source I_0 (laser with a wavelength of 635 nm in the present work) is expanded through a beam expander and filtered by an interferometric pass-band filter. By means of the measured intensity I, it is possible to calculate the transmittance. According to Lambert-Beer law, low transmittance values means high value of light absorption due to high particles concentration or high optical path (i.e. the central part of flame). The maximum of absorbed portion of light is 16% in the center top part of flame where the optical depth of soot is higher. The reduction of LII signal is about half of absorption (about 8%) as emitting soot is positioned in the center of flame. To calculate a correct flame temperature and subsequently a coherent value of f_v, both red and blue signals were corrected by self-absorption errors. The specific extinction coefficient for carbonaceous aggregates at 488 nm is about 20% more than at 635 nm, as suggested by some authors [27, 28, 29, 30] if the carbon density and the flame geometry remain the same.

4. RESULTS AND DISCUSSIONS

After images treatment, calibration and corrections, heated soot temperature behaviour in time was calculated through equation 2. The averages of the calibrated images for red and blue acquisitions for each acquisition time were considered. For time steps up to 1010 ns, temperature is about the local flame temperature. The maximum of time resolved temperature corresponds to the incipient sublimation of soot. At this time (30ns of Figure 2), it can be assumed that the soot particles do not modify theirs dimensions and that the intensity is proportional to soot volume fraction [6]; so the f_v calculated at this time by means of equation 4 is the volume fraction of the laminar diffusion flame into thermodynamic equilibrium conditions. The temperature and the soot volume fraction into two dimensions was obtained by a pixel-to-pixel calculation on the blue and red averaged images. Figure 5 shows the corrected LII signal (on left), the temperature of soot (on center) and the volume fraction fv calculated at the maximum of LII curve (see Figure 2).

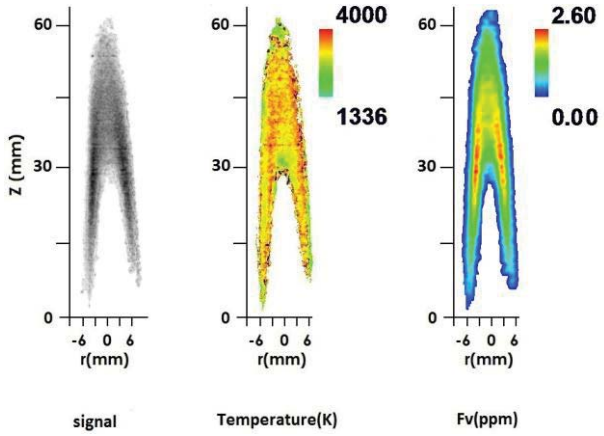

Figure 5: Flame images of LII signal(on left), the temperature (on center) and the volume fraction *Fv* (on right) of soot

Temperature image shows region in the central part of flame where temperature remain almost constant near the sublimation temperature, as confirmed by De Iuliis [25]. However the highest temperature values can be found near the edges. The maximum value of temperature is about 4000K while about the 75 % of flame surface lies in the

temperature range between 3500 K and 3800 K. This results is in agree with the LII theory according which soot particles, in low fluence condition, are heated below sublimation temperature independently by theirs dimension [22]. In this condition and before the soot sublimation, it is correct to assume that the soot volume fraction is related to soot concentration at steady state. As reported in Figure 5 on right for the soot volume fraction, a high concentration (about 2.6ppm) is detectable in the center part, near borders of flame. Due to the reduced width of the laser sheet, it can be assumed that the acquired signal corresponded to the radial flame profile and not to an integral of light collected along the optical path [31]. Images alignment is fundamental for a 2D temperature and subsequently soot volume fraction visualization. An incorrect flame position of red acquisitions with respect to blue ones leads to incoherent values. As blue filtered images are less intense in terms of corrected LII signal, in the peripherals zone of the flame there is no overlapping between red and blue signals where there is a low signal-to-noise ratio. In this zone a null value was imposed for the calculated parameter. Soot emitting temperature and volume fraction has been calculated by a pixel-to-pixel analysis staring from two color laser induced incandescence averaged images ratio. This analysis has been used to determine the 2D−LII time resolved behaviour using a three dimensions array of pixels, in which rows and columns are flame temperatures for a single time step and pages are calculated temperature at different instants. The temperature variation in time has been obtained by referring to a single pixel coordinate thus an exponential curve has been obtained for each pixel. The primary soot diameter has been calculated from the decaying part of temperature curve using equation 4. As regard surrounding gas temperature determination for soot temperature decay, flame temperature was calculated through the Two Color method. This technique is based on the acquisition of blackbody radiation of soot at two different wavelength [33, 34] In Figure 6 on left, a bi-dimensional primary soot behaviour applying the procedure proposed by [17] has been reported.

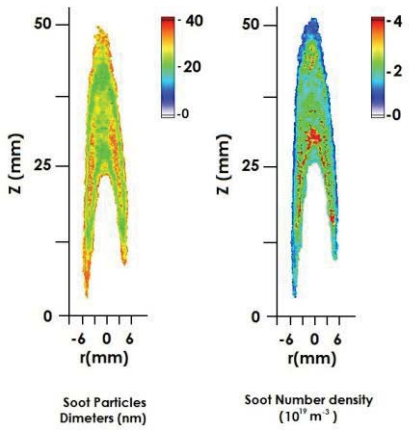

Figure 6: Behaviour of particles primary diameters in nm on left and particle density number (10^{19} m^{-3}) on right.

The maximum of primary soot diameters (about 20-30 nm) is located in the bottom part and in queues of flame where the soot concentration is high (see Figure 5 on left). Results are in good agreement with other researchers results for 1D calculation of primary particles diameters [1,35]. In the upper part of flame there is no overlapping between LII red and blue images and a negative exponential factor of equation 4 is obtained. In these points a wrong diameter value are calculated and so a null value was imposed. Primary particles concentration into the sampling volume was calculated knowing the primary diameters of particles. In Figure 6 soot number density is reported. High values of soot number density reached in the central bottom part of flame, while a decreasing behaviour is detectable from center to the edge of flame. Results obtained for normalized primary particles diameter and density number are in good agreement with values and trends obtained from others researchers [36, 37] using a photodiode as acquisition system. A mean diameter of 33 nm with a standard deviation σ of 1.1 has been obtained.

5. CONCLUSIONS

In the present work a two dimensions time resolved laser induced incandescence technique was proposed as detection system for soot primary dimension measurements into a LGP laminar diffusion flame. Two color laser induced incandescence was used to calculate the heated soot particles temperature with two interchangeable pass band filters at 488 nm and 635 nm. A series of 50 images for 21 different time step were acquired by means of a water cooled intensified CCD. A hardware calibration was perform to correlate acquired signal with emitted power by soot heated particles. Self-absorption of soot in flame and laser energy loos during flame crossing were corrected to rescale the LII signal and to obtain a symmetric radial profile of flame. It was found that these two factors can affect the temperature and fv results of about the 12% error which cannot be neglected in case of a quantitative measurement. Although laminar diffusion flame is stationary, flame position into images could be different due to local air fluctuations and to the difference in light intensity between the two filters. A low pass FFT filter and an adjacent point smoothing was applied to images to reduce flame noise. An appropriate alignment and orienting algorithm was developed to grant two colour images overlapping. The algorithm was developed on the basis of flame mass center position. This accuracy in imaging manipulation allows a pixel-to-pixel volume fraction calculation. A decaying curve of the incandescence signal and temperature was obtained from images acquired at different time instant. The soot primary particles diameter and the density number has been calculated for the entire flame starting from the decay of signal in a bi-dimensional domain.

6. REFERENCES

[1] F. Xu, A. El-Leathy, C. Kim, G. Faeth, Soot surface oxidation in hydrocarbon/air diffusion flames at atmospheric pressure, Combustion and Flame 132 (2003) 43-57.

[2] J. Reimann, S. Kulhmann, S. Will, 2d aggregate sizing by combining laser-induced incandescence (LII) and elastic light scattering (ELS), Applied Optics-B (2009) 853-892.
[3] T. Allen, Particles Size Measurements, 1990.
[4] B. H. Kaye, Direct Charicaterization of Fineparticles, 1981.
[5] C.R. Shaddix, K.C. Smyth, Laser-induced incandescence measurements of soot production in steady and flickering methane, propane, and ethylene diffusion flames, Combustion and Flame 107 (1996) 418 -452.
[6] L. Melton, Soot diagnostic based on laser heating, Applied Optics (1984),2201–2208.
[7] R. L. Vander Wal, Laser-induced incandescence: detection issues, Appl.Opt. 35 (1996) 6548-6559.
[8] A. Boiarciuc, F.Foucher, C.Mounam-Rousselle, Soot volume fractions and primary particle size estimate by means of the simultaneous two-color-time-resolved and 2d laser-induced incandescence, Applied Physics B 83 (2006) 413-421.
[9] D.Snelling, G.Smallwood, O.Gulder,W.Bachalo, A calibration-indipendent technique of measuring soot by laser-induced incandescence using absolute light intensity, in: The Second Joint Meeting of the US section of the Combustion Institute, 25-28 Marc 2001, Oakland, California.
[10] B. Axelsson, R. Collin, P. Bengtsson, Laser-induced incandescence for soot particle size and volume fraction measurements using on-line extinction calibration, Applied Physics B Lasers and Optics 72 (2001) 367-372.
[11] R.Wainner, J.Seitzman, Soot diagnostics using LII in flames and exhaust flows, AIAA Jour. (1999).
[12] D.R.Snelling, G.J.Smallwood, O.L.Gulder, Absolute intensity measurements in laser induced incandescenc, 2000.
[13] J. V. Pastor, J. M. Garca, J. M. Pastor, J. E. Buitrago, Analysis of calibration techniques for laser-induced incandescence measurements in flames, Measurement Science and Technology 17 (2006).
[14] O. Harang, M. Kosch, Absolute optical calibrations using a simple tungsten bulb: Theory, Sodankyla Geophysical Observatory Publications 92 (2003) 121-123.
[15] W. Dalzel, A. Sarofim, Optical constants of soot and their application to heat-flux calculations, J. of Heat Transfer 91 (1969) 100-104.
[16] B. McCoy, C.Cha, Transport phenomena in the rarefied gas transition regime, Chem. Eng. Sci. 29 (1974) 381-388.
[17] O. Leroy, J. Perrin, J.Jolly, M. Palat, M. Lefebvre, Thermal accommodation of a gas on a surface and heat transfer in cvd and pecvd experiments, Journal of Physics D: Applied Physics 30 (1997) 499-509.
[18] H. Bladh, P. Bengtsson, Characteristic of laser induced incandescence from soot in studies of time-dependent heat and mass-transfer model, Applied Physics B-Lasers and Optics 78 (2004) 241-248.
[19] P. Rosenkranz, M. Matus, M. L. Rastello, On estimation of distribution temperature, Metrologia 43 (2006) S130.
[20] R. Larrabee, The spectral emissivity and optical properties of tungsten, Massachusetts Institute of Technology, Research Laboratory of Electronics, 1957.
[21] C. Schulz, B. Kock, M. Hofmann, H. Michelsen, S. Will, B. Bougie, R. Suntz, G. Smallwood, Laser-induced incandescence: recent trends and current questions, Applied Physics B 83 (2006) 333-354.
[22] D. J. Bryce, N. Ladommatos, H. Zhao, Quantitative investigation of soot distribution by laser-induced incandescence, Appl. Opt. 39 (2000) ,5012-5022.
[23] J. Wolberg, Data analysis using the method of least squares: extracting the most information from experiments, Springer, 2006.
[24] R.Dobbins, G.Mulholland, N.Bryner,Comparison of a fractal smoke optics model with light extinction measurements, Atmospheric Environment 28 (1994) 889-897.
[25] I. Colbeck, B. Atkinson, Y. Johar, The morphology and optical properties of soot produced by different fuels, Journal of Aerosol Science 28 (1997) 715-723.
[26] Nishida, Osami, Mukohara, Seiya, Optical measurements of soot particles in a laminar diffusion flame, Combustion Science and Technology 35 (1983) 157-173.
[27] E. Patterson, R. Duckworth, C. Wyman, E. Powell, J. Gooch, Measurements of the optical properties of the smoke emissions from plastics, hydrocarbons, and other urban fuels for nuclear winter studies, Atmospheric Environment. Part A. General Topics 25 (1991) 2539-2552.
[28] D. Snelling, G. Smallwood, I. Campbell, J. Medlock, O. Gulder, Development and application of laser induced incandescence (lii) as a diagnostic for soot particulate measurements, in: AGARD 90th Symposium of the Propulsion and Energetics Panel on Advanced Non-Intrusive Instrumentation for Propulsion Engines, 20-24 October 1997, Brussels, Belgium.
[29] H.C.Hottel, F.P.Broughton, Determination of true temperature and total radiation from luminous gas flames, Ind. and Eng. Chem. Analytical Edition 4 (1932) 166–175.